THE MODEL OF THE "INTERACTIVE PLASTIC HINGE"

M. Iványi

Department of Steel Structures,
Technical University, H-1521 Budapest

Received September 26, 1984

Abstract

Instead of the plastic hinge the "interactive hinge" and "zone" have been introduced for a mounting base constructed from plates which are of a much higher degree of freedom than the previous ones as they also embrace the effects of strain hardening of the steeel material, of the residual deformation, as well as of the plate buckling bringing about the "descending" characteristics. The traditional plastic hinge is only suitable to take the rigid and ideally plastic state from among the stability features into account.

1. Introduction

A usual simplifying assumption at investigating the plastic load capacity of steel structures is to substitute the member unit sections of the mounting in elastic-plastic state by an ideal mounting base with its section bearing the highest load in a completely plastic state and its remaining parts in a completely elastic state. Further simplification can be achieved by regarding the mounting as of rigid-plastic material.

The part of the mounting idealized as above is called a plastic hinge, a concept of great importance in calculating the plastic load capacity of steel structures. The concept and term are due to Gábor Kazinczy [1].

The concept of the plastic hinge is primarily related to the load-displacement relationship at bending, but it can also be applied at other types of load.

The basic models of the plastic hinge may be taken as *elementary* or *finite*, so-called *plastic zones.*

The investigation of the critical state of limitless plastic deformation in steel structures is greatly simplified by the introduction of the plastic hinge, however, the model of the plastic hinge involves numerous approximations and neglections as regards the steel material. The nature and effects of these approximations and neglections have been continually analyzed by researchers since investigations of plastic theory of structures had developed (Beedle [2]). In the past decades several approximations and neglections formulated in the model of plastic hinges have been investigated. These investigations facilitated studies which, in part retaining the concept of the plastic hinge, related to effects due to the properties of steel material and which resulted in a good correspondence between the theoretical load bearing capacity and behaviour of steel structure and the experimental results and experiences. From among these, two effects important in our investigations will be shown to be taken into account, namely the strain-hardening as well as the residual stresses.

The behaviour of the member unit, the cross section and thus that of the plastic hinge is influenced by stability phenomena as well such as disadvantageous changes (bucklings) in the cross section geometry.

In the following, the effects of changes in the cross section geometry of compressed and bending members will be discussed. It will be assumed that the rod is already in a plastic state and the bucklings of the units forming the cross section hinder the development of plastic deformations. The task is to determine the yield mechanism curve due to the bucklings in the plates forming the members.

2. The effect of strain-hardening and residual stresses on the load-displacement relations of member units

2.1. The methods have emerged for taking the effect of strain hardening of steel into account:

1) hardening plastic hinge;
2) hardening plastic zone.

1) The *hardening plastic hinge* is an expansion of the concept of the traditional plastic hinge. The bending moment in the hinge can be written as

$$M = M_p + \alpha\Theta$$

where α is a function of the material characteristics and of the shape of the bending moment diagram;

Θ is the angle of rotation by the hardening plastic hinge.

Horne [3] has suggested a "rigid-plastic-rigid" hinge model for taking the effect of strain hardening into account (Fig. 1).

It follows from the considerations that

$$m = M_p \left(\frac{b}{2fh}\right)\left(\frac{E}{k\sigma_Y}\right)\Theta$$

and taking into account that

$$\frac{b}{2} = \frac{I}{W}; \quad M_p = f \cdot W \cdot \sigma_Y$$

$$m = \frac{EI}{kh}\Theta = \alpha\Theta$$

Further improving Horne's "rigid-plastic-rigid" hinge model, Horne and Medland [4] developed a "rigid-plastic-hardening" hinge model. The σ—ε diagram employed is shown in Fig. 2 whereas the following formula was derived for m:

$$m = M_p \frac{x}{h} = M_p \left\{ \sqrt{\left[\left(\frac{k}{\bar{K}} \right)^2 + 2 \left(\frac{b}{2fh} \right) \left(\frac{E}{\bar{K} \sigma_Y} \right) \cdot \Theta \right]} - \frac{k}{\bar{K}} \right\}$$

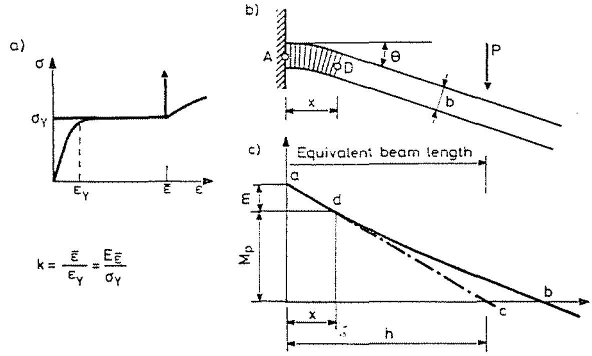

Fig. 1

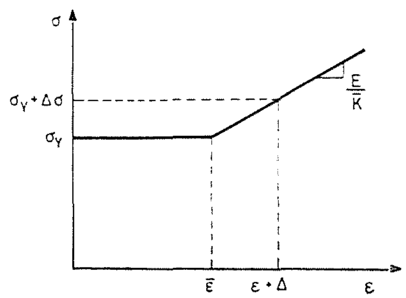

Fig. 2

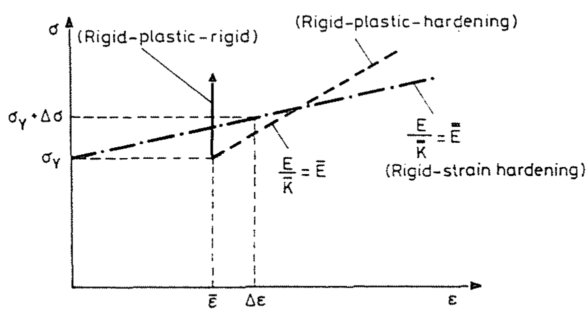

Fig. 3

Meyer and Gerstle [5] used a "rigid-hardening" hinge model in their investigations. They calculated the hardening modulus from a moment-rotation diagram determined experimentally. Let us investigate the moment-rotation relationship of a "rigid-hardening" plastic hinge. The σ—ε diagram shown in Fig. 3 is employed. In cross section A (Fig. 1.b) $\sigma_Y + \Delta\sigma$ and $\Delta\varepsilon$ as well as

$$\Delta\sigma = \frac{E}{\overline{\overline{K}}} \Delta\varepsilon$$

The curvature in cross section A is

$$\varkappa_A = \frac{\Delta\varepsilon}{\frac{b}{2f}}$$

In cross section D the curvature is $\varkappa_D = 0$. Assuming the variation between cross sections D and A to be linear, the mean value of the curvature is taken. Hence, the rotation of the hinge is

$$\Theta = \frac{\frac{1}{2}\Delta\varepsilon}{\frac{b}{2f}} x = \frac{\Delta\varepsilon f}{b} x$$

From the moment diagram (Fig. 1.c)

$$\frac{m}{M_p} \simeq \frac{x}{h} = \frac{\Delta\sigma}{\sigma_Y} = \frac{E}{\overline{\overline{K}} \cdot \sigma_Y} \cdot \Delta\varepsilon$$

and hence

$$\Delta\varepsilon = \frac{\overline{\overline{K}} \cdot \sigma_Y}{E} \cdot \frac{x}{h}$$

and

$$\Theta = \frac{f\,\overline{\overline{K}} \cdot \sigma_Y}{Eb} \frac{x^2}{h}$$

$$x = \sqrt{\left(\frac{bh}{f}\right)\left(\frac{E}{\overline{\overline{K}} \cdot \sigma_Y}\right) \cdot \Theta}$$

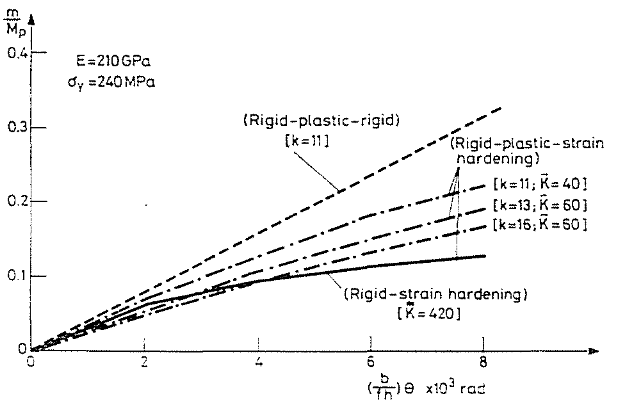

Fig. 4

therefore

$$m = M_p \sqrt{\left(\frac{b}{fh}\right)\left(\frac{E}{\overline{\overline{K}} \cdot \sigma_Y}\right) \cdot \Theta}$$

The behaviour of the different hardening plastic hinges is shown in Fig. 4.

The σ—ε diagram of steel material is best approximated by the σ—ε diagram used at the "rigid-plastic-hardening" model, however, the use of the "rigid-plastic-hardening" model is rather difficult.

The application of the "rigid-hardening" model is relatively simple and, by varying the parameter $\varkappa$, the model behaves similarly to the "rigid-plastic-hardening" model.

2) The model of the *hardening plastic zone* yields a physically more accurate description of the effect of hardening since it assumes the hardening to develop in a mounting section of finite length.

Roderick [6] was the first to investigate the effect of the hardening zone, he carried out his investigations on the basis of a σ—ε diagram determined experimentally.

It has been known since the work of Lay [7] that without the assumption of a hardening zone the inelastic displacements of supporting structures cannot be determined.

The moment-curvature relationship of an elastic ideally plastic material beam is shown in Fig. 5. It is shown by the moment diagram of the two-support beam loaded by a concentrated force as well as by the diagram of the relative rotations (curvatures) indicated along the beam that the inelastic displacements are indeterminate. The example in Figs 5.c and d indicates that the moment under the concentrated force may be higher than the breaking moment M_p as well as that the inelastic displacement can be determined.

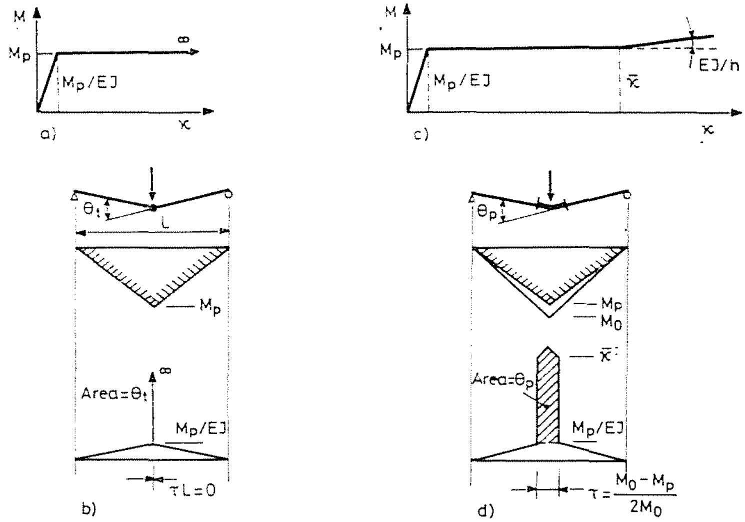

Fig. 5

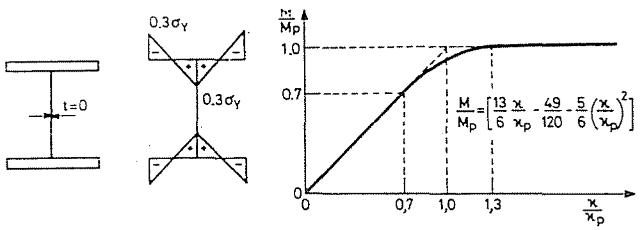

$$\frac{M}{M_p} = \left[\frac{13}{6}\frac{x}{x_p} - \frac{49}{120} - \frac{5}{6}\left(\frac{x}{x_p}\right)^2\right]$$

Fig. 6

Tranberg et al. [8] employed an investigation method which applied a "three-line" moment-curvature relationship. In the first phase the elastic, in the second the plastic and in the third the hardening effect was taken into account.

2.2. The importance of *residual stresses, deformations* has been recognized by research for about the last seventy years. Numerous theoretical and experimental investigations have been carried out in the field.

The effects of residual stresses and deformations have been summarized by Lay [9]. Several factors influence the development of residual stresses, deformations and the research work concerning their magnitude and distribution is not yet concluded. Their effect taken into account in our investigations is illustrated by an example (Fig. 6) assuming that the web of the I-section plays but the role of a distance piece. The moment-curvature diagram passes after a relatively small elastic section into a transitional curve and then attains the value of the plastic moment M_p. The effect of the residual stress is primarily significant at the transition between the elastic and plastic states.

3. A review of the literature concerning the investigation of the yield mechanism curve

The "final" deteriorated form of cylindrical shells pressed in axial direction, the so-called Yoshimura-configuration which evolves from cylinder jacket pieces through the development of planar triangle pieces, is well known. Mallock [10] was among the firsts to describe the development of this type of deformation.

Haaijer [11] assumed the plate buckling problem to be solvable as bifurcation of equilibrium. Ben Kato [12] approached the problem from another angle.

In case of real plates, if the thickness-width ratio is small enough, fine "crumplings" (waviness) can be observed at the beginning of the yield. The plate does not immediately lose its load bearing capacity, it can take the load causing the yield up to a certain deformation. This "crumpling" can actually be regarded as a kind of yield mechanism.

One of the main deficiencies of Ben Kato's model is that the bucklings in the plates forming the I cross section develop — by assumption — in a way geometrically independent of each other.

Climenhaga and Johnson [13] employed the yield mechanism at the investigation of the buckling of steel beam parts of composite steel concrete construction due to a negative moment.

Korol and Sherbourne [14] undertook the buckling investigation of square cross section tubes by theoretical and experimental methods. The investigation was concerned with the post-critical behaviour of plates buckling in elastic state.

Murray [15] employed the yield mechanism curve at the investigation of ribbed compressed plates which has been further developed by Walker and Murray [16].

Davies, Kemp and Walker investigated the behaviour of compressed plates supported by a hinge along their unloaded sides [17] also accounting for the effect of normal and shearing stresses occurring in linear plastic hinges.

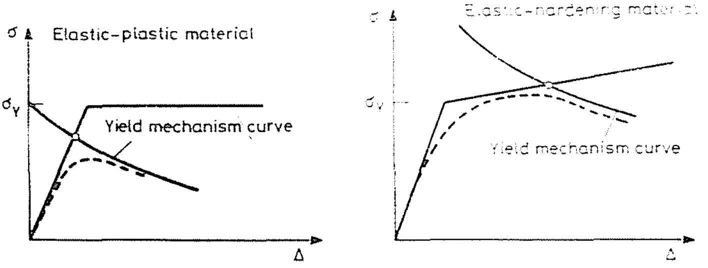

Fig. 7

The effect of bucklings developing at the connections of rectangular tubes was also studied with the aid of the yield mechanism curve (Mouty [18]; Packer, Davies [19]).

Iványi [20, 21] undertook the buckling investigation of compressed and bending bars with the aid of the yield mechanism curve.

The models employed in the literature can be divided into two groups; to the one belong the investigations that assume an elastic-ideally plastic material (Korol, Sherbourne, Murray, Walker, Davies, Kemp [14—17] while to the other those where also the effect of strain-hardening has been taken into account (Ben Kato, Climenhaga, Johnson, Iványi) (Fig. 7).

4. Investigation of plate buckling with the aid of yield mechanism

4.1. *Assumptions*

In the course of plate experiments, if the thickness–width ratio is small the plate does not lose its load bearing capacity with the development of plastic deformations but is able to take the load causing yield until a deformation characteristic of the plate occurs and is even able to take a small increase in load. In the course of the process "crumplings" (bucklings) can be observed on the plate surface. These "crumplings" form a yield mechanism with the plastic moments acting in the linear plastic hinges (peaks of waves) not constant but ever increasing due to strain-hardening. The yield mechanism formed by the "crumplings" extends to the component plates of the bar. The description of its behaviour is obtained, from among the extreme values theorems of plasticity, with the aid of the *theorem of kinematics*.

Thus, in the course of our investigations an upper limit of the load bearing has been determined, however, to be able to assess the results, the following have to be taken into consideration: on the one hand the yield mechanisms are taken into account through the "crumpling" forms determined by experimental results and on the other hand, the results of theoretical investigations are compared with those of the experimental investigations.

4.2. *Yield mechanism forms based on experimental results*

The different form of yield mechamisms can be determined on the basis of experimental results.

The yield mechanism forms of an I-section bar can be classified according to the following criteria:

a.) according to the manner of loading,

b.) according to the positions of the intersecting lines of the web and the flanges, the so-called "throat-lines", thus

bi.) the evolving formation is called a planar yield mechanism if the two

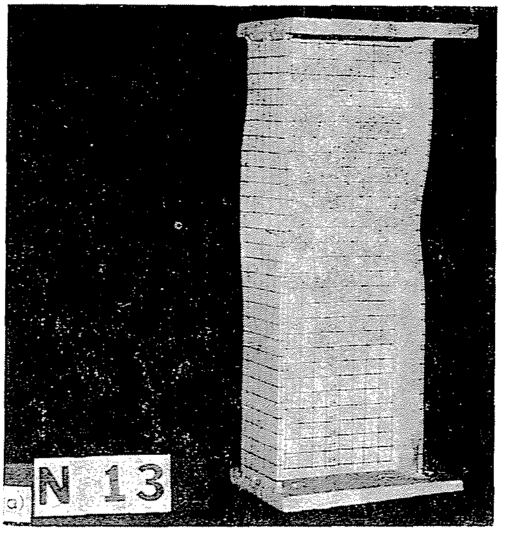

Fig. 8. a

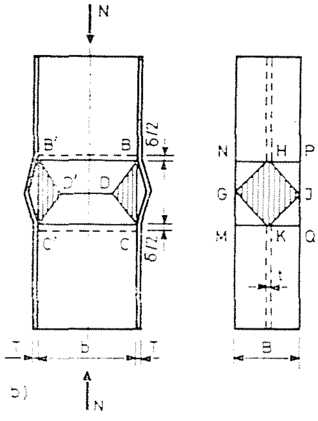

Fig. 8. b

"throat-lines" are in the same plane also after the development of the yield mechanism.

bii.) the evolving formation is called a spatial yield mechanism if the two "throat-lines" are not in the same plane after the development of the yield mechanism.

4.21. *Yield mechanisms of compression members*

(i) Planar yield mechanism

The buckled form of the compression member is shown in Fig. 8.a, while the formation of the chosen yield mechanism in Fig. 8.b.

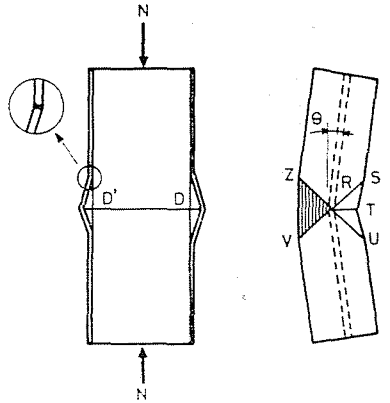

Fig. 9

Plastic deformation occurs in the shaded regions.

As an effect of compressive force N a compression develops.

The symbol of the yield mechanism is $(N)_P$ where P stands for the planar yield mechanism formation.

(ii) Spatial yield mechanism

The formation of the spatial yield mechanism for a compression member is shown in Fig. 9. The ends of the member are assumed to be hinge-supported in both main inertia directions. The yield mechanism that has occurred is called spatial, the phenomenon models the planar buckling of the compression member or the buckling of the component plates in the course of buckling.

The symbol of the yield mechanism is $(N)_S$ where S stands for the spatial yield mechanism formation.

4.22. *Yield mechanisms of bent members*

a.) In case of a bending moment constant along the member axis:

ai) planar yield mechanism

The buckled form of the bent specimen is shown in Fig. 10.a, while the chosen yield mechanism formation in Fig. 10. b. As an effect of moment M a rotation ϑ develops.

As an effect of M, tension and compression parts develop.

The symbol of the yield mechanism is $(MC)_P$, where C stands for the constant bending moment.

aii) Spatial yield mechanism

The form of the spatial yield mechanism in the case of a bent rod is indicated in Fig. 11. The rod ends are assumed to be hinge-supported both main inertia directions. The yield mechanism models the buckling of the component

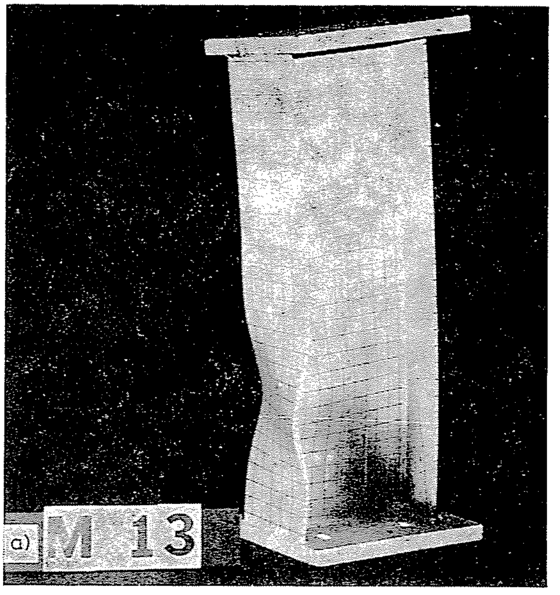

Fig. 10. a

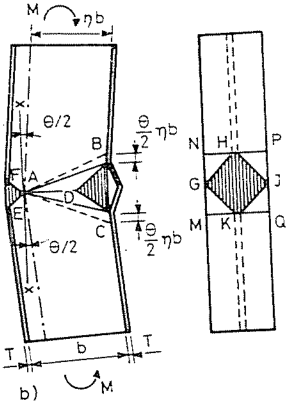

Fig. 10. b

plates of the bent member, the lateral buckling of the beam as well as their interaction.

The buckled formation of a double-support beam specimen is shown in Fig. 12.a, while the chosen yield mechanism formation in Fig. 12.b.

In case of the yield mechanism formations in Fig. 12 the effect of neighbouring supports (the effect of ribs) has also been taken into account. As an effect of the moment, a rotation Θ develops.

The symbol of the yield mechanism is $(MC)_S$.

b.) In case of a bending moment varying along the rod axis.

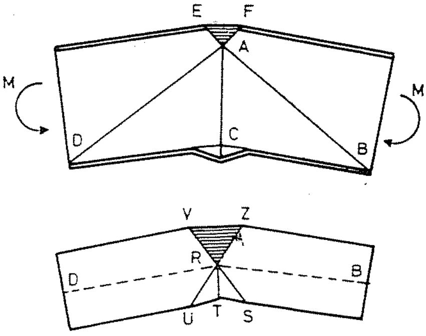

Fig. 11

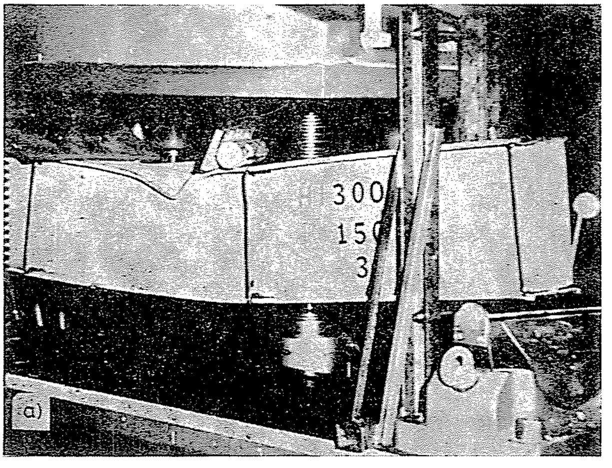

Fig. 12. a

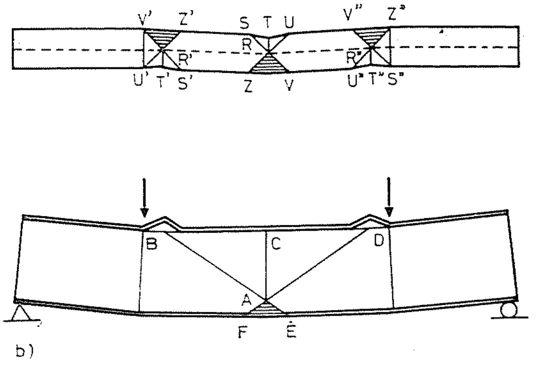

Fig. 12. b

In case of a varying bending moment along the member axis it is assumed that the "crack" of the web plate of the I-section in the cross section of the concentrated force is hindered by the suitable thickness of the web plate or by the ribs.

Climenhaga, and Johnson [13] assumed yield mechanism forms similar to those introduced in point (b) for the investigation of bucklings occurring at the steel beam parts of composite steel-concrete construction.

bi) Planar yield mechanism:

The buckled form of a bent specimen is shown in Fig. 13.a, while the selected yield mechanism in 13.b. As an effect of the moment a rotation Θ develops (Fig. 13).

Because of the clamping of the cross-section EC, the yield mechanism loses its symmetric character.

The symbol of the yield mechanism is $(MV)_P$ where V stands for the varying moment.

bii) Spatial yield mechanism

The form of the spatial yield mechanism in case of a bending moment varying along the rod axis is shown in Fig. 14.

As an effect of the moment a rotation Θ develops.

The symbol of the yield mechanism is $(MV)_S$.

4.3. *Yield mechanisms of the component plates of an I-section member*

Yield mechanism formations have been determined for different stresses. On the basis of the experimental results it is expedient to decompose these yield mechanism formations to the yield mechanism formations of the component plates of an I-section rod as certain component plate formations appear in other yield mechanisms, too.

To classify the yield mechanisms of component plates, the following division has been used:

a.) flange plate, if the plate is supported along the central line,

b.) web plate, if the plate is supported at the unloaded ends.

Fig. 15 shows the yield mechanisms of the component plates where F is the flange plate, W is the web plate, the odd numbers refer to the planar yield mechanisms while the even ones to the spatial yield mechanisms.

4.4. *"Joining" the yield mechanisms of component plates*

The "joining" of the yield mechanisms of component plates depends on the positions of the so-called "throat-lines" of the yield mechanism chosen on the basis of the experimental results.

In cases pertaining to planar yield mechanisms this "joining" is to be realized in a linear way, with a linear plastic hinge: the length of the linear

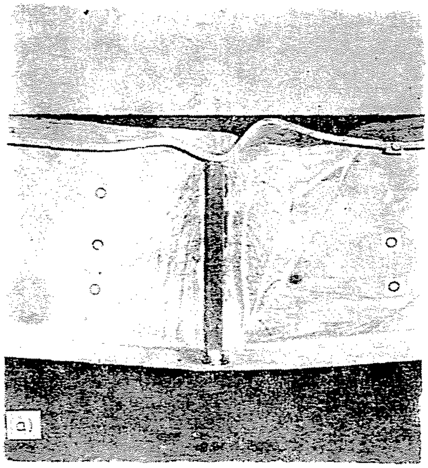

Fig. 13. a

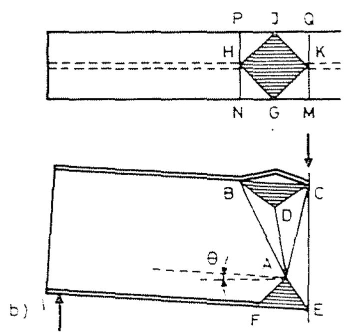

Fig. 13. b

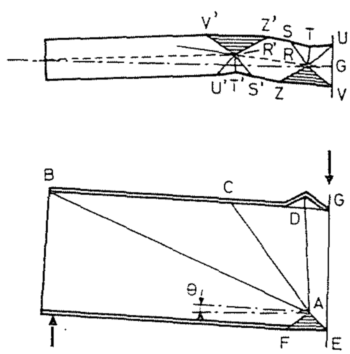

Fig. 14

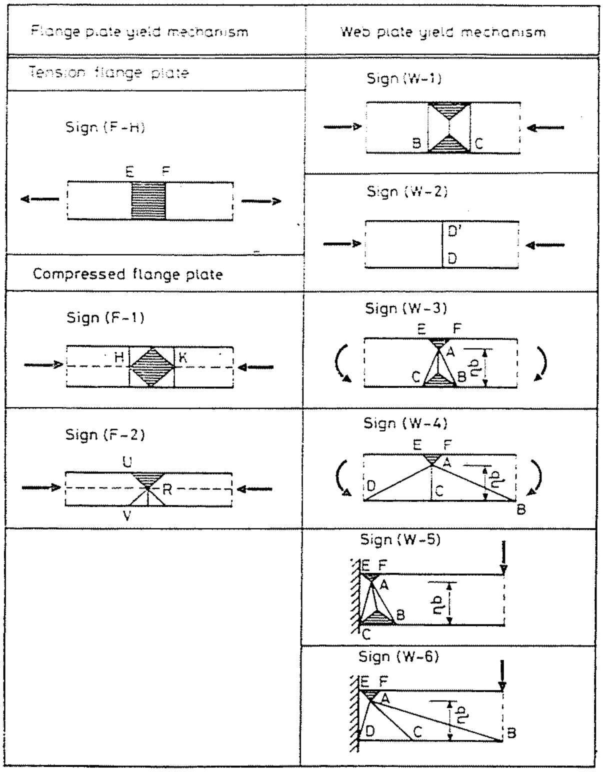

Fig. 15

plastic hinge is governed — due to the properties of the chosen yield mechanism — by the length of the yield mechanism of the compression flange plate (*F*-1). In case of spatial yield mechanisms the "joining" should be realized in one point or more points.

The relationships of the component plate yield mechanisms and the "joining" of the component plates have been given by Iványi [22]; references [20] and [21] show the basic relationships of partial cases.

5. Comparison of experimental and theoretical results

The determination of the yield mechanism curve has been carried out by assuming a particular yield mechanism formation. The determination of this formation was primarily enabled by experimental results, thus, for the comparison of theoretical and experimental results the following had to be analyzed:

— on the one hand, the relation between the computed and measured load-displacement curves,

— on the other hand, the relation between the assumed formation and the buckling form obtained from the experimental results.

The basis of the comparison of experimental and theoretical investigation results were compression bent and eccentrically compression members as well as so-called "control"-beams.

5.1. *Investigation of the results of compression members*

Because of the arrangement of the specimens, the end-support is clamped from the point of view of bending and torsion to the so-called "weak" axis and the evolving yield mechanism is a planar one, its symbol is $(N)_P$.

The four load-displacement curves determined on the basis of the experimental results are shown in Fig. 16.

Here:

$$N_p = 2BT\sigma_{YF} + bt\sigma_{YW}$$

$$\delta_p = \frac{N_p \cdot L}{E \cdot A}$$

The relation and coincidence of the experimental and theoretical results is acceptable.

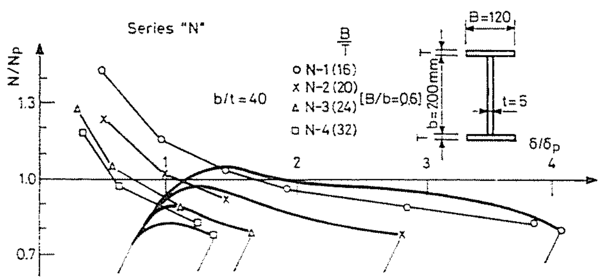

Fig. 16

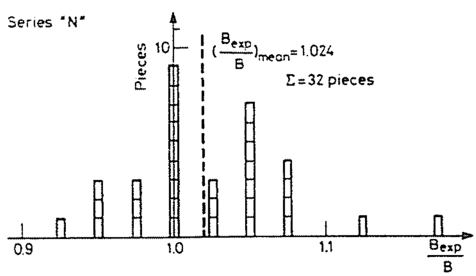

Fig. 17

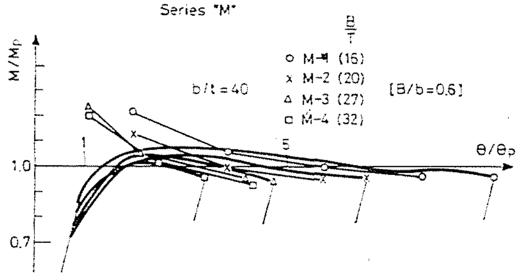

Fig. 18

Figure 17 indicates the results of measurement of forms evolving as an effect of plate buckling that served to disclose the form of buckling of the flange plate. The bucklings of the component plates are in interaction with each other and thus it is sufficient to investigate the buckling formation of the flange plate. The assumed buckling form of the flange plates has a length B (Fig. 18.b) the diagram compares the measured buckling wave lengths $(B)_{\exp.}$ to the width B of the flange plate. It can be observed that the assumed yield mechanism formation coincides with that obtained from the experimental results.

5.2. *Investigation of the results of bent specimens*

The buckling investigation of component plates of bent beams can also be carried out with the aid of the yield mechanism curve.

Because of the arrangement of the specimens the evolving yield mechanism is a planar one, its symbol is $(M)_P$.

The load-displacement curves determined on the basis of the experimental results fit to the curve determined with the aid of the yield mechanism (see Fig. 18).

Here:

$$\Theta_p = \frac{M_p \cdot L}{2E \cdot I_x}$$

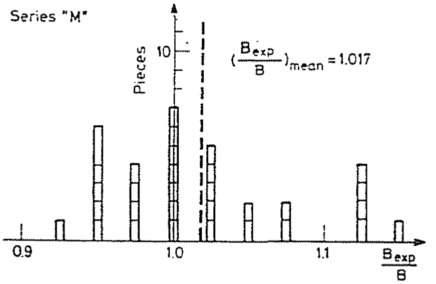

Fig. 19

Figure 19 shows the results of measurement of the form developing as an effect of plate buckling. The diagram contains the results of measurements realized on the buckling form of the compression flange plate (Fig. 10.b) and it can be seen that the assumed yield mechanism formation coincides with the form obtained from the measurement results.

5.3. *Investigation of the results of welded I-section beams ("Control" beams)*

5.31. *Investigation of the results of beams bent with varying moment*

In case of a varying moment diagram plate bucklings appear first of all. The beam section has been selected to be short enough to obtain a planar yield mechanism, i.e. the so-called "throat-lines" are in the same plane after loading, too. The symbol of the yield mechanism is $(MV)_P$.

Figure 13.b indicates the yield mechanism formations while Fig. 20 indicates the theoretical and experimental results (load-displacement curves).

5.32. *Investigation of the results of beams bent with a constant moment*

In case of beams bent with a constant moment, the so-called beam rotation occurs, first of all, because of the support conditions, namely the two "throat-lines" were not in the same plane after loading and the cause of the final deterioration was plate buckling in this case, too.

Figure 12.b shows the selected yield mechanism formation, its symbol is $(MC)_S$.

Figure 21 indicates the experimental results as well as the results of theoretical investigations obtained by assuming a yield mechanism.

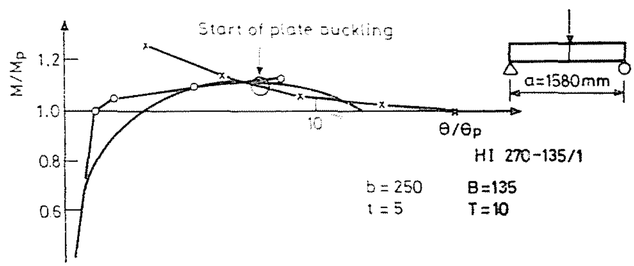

Fig. 20

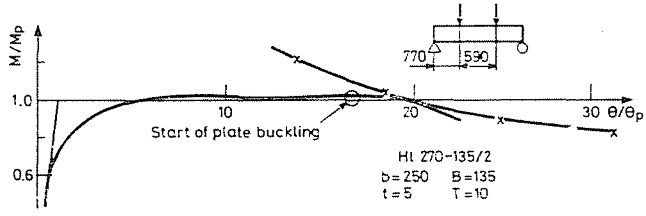

Fig. 21

It can be observed that the yield mechanism curves determined on the basis of the experimental results describe well the "descending" part of the load-displacement curve and also that the yield mechanism formation coincides with the one obtained from the experimental results. Hence, the yield mechanism curves are suitable to determine the stress-displacement relationships of the member elements by taking into account both the effect of plate buckling and lateral buckling.

6. Models of stress-displacement (relative displacement) of I-section members

The plastic load-bearing investigation assumes the development of rigid — ideally plastic hinges, however, the model describes the inelastic behaviour of steel structures but with major constraints and approximations. In section 2 we introduced the major effects with the consideration of which the behaviour of the steel material and the I-section member can be taken into account in a more realistic way.

i) When determining the load-displacement (relative displacement) relationship of I-section member, the symbol of the elastic state is E and if the so-called "rigid" state is assumed instead of the elastic one, the symbol of the rigid state is R.

ii) The effect of residual stress and deformation is characterized by a straight line for the sake of ease of handling. The symbol used when taking the residual stress and deformation into consideration is O.

iii) Strain-hardening is one of the important features of the steel material, S indicates that it had been accounted for.

iv) In section 4.4. the effect of buckling of the I-section member component plates on the rod element load-displacement relationship has been investigated, this is indicated by L.

The models that take the above effects into consideration at the investigation of the load-displacement (relative displacement) relationship of I-section are called "interactive" ones.

6.1. *The model of the R—O—S—L interactive hinge*

The model of the interactive hinge taking into consideration the effect of rigid — residual stress — strain hardening — plate bucklings can be described with the aid of the "equivalent beam length" suggested by Horne [3] (Fig. 22.a). The material model employed at the investigations is shown in Fig. 22.b. The effect of the residual stresses and deformations is substituted by a straight line. The effect of strain hardening can be determined with the help of the rigid-hardening (R—S) model introduced in section 2. The buckling of

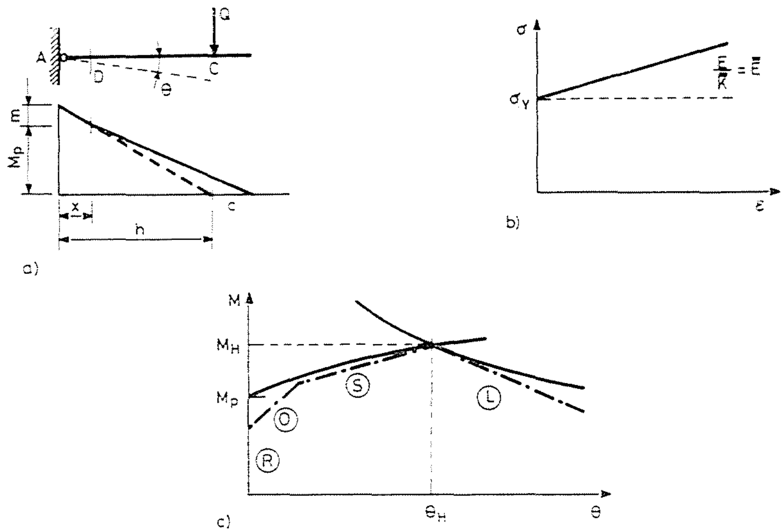

Fig. 22

the I-section member component plates is described by the yield mechanism curve which is substituted by a straight line.

Figure 22.c indicates the load-displacement relationship belonging to the (*R—O—S—L*) interactive hinge. The substitution by straight lines is justified to simplify the investigations. In the (*R—O—S*) sections the intersections are connected while in section *L* the moment rotation relationship is substituted by a tangent that can be drawn at the apex.

6.2. *The model of the R—S—L interactive "zone"*

It was Lay [9] who drew attention to the phenomenon that an inelastic hinge contracted into a single cross section cannot suitably model the displacements of a structure and thus it seems expedient to assume the inelastic state in a finite zone.

In our investigations the effect of finite zones can be determined with the aid of the load-relative displacement curve and the moment diagram obtained for an I-section rod element. Figure 23.a shows the beam under investigation. The moment-curvature relationship pertaining to cross section *A* can be determined easily with the hardening effect taken into account. Figure 23.c shows a situation with $M_p < |M| < M_H$) while Figure 23.d the state belonging to $|M| = M_H$. The omission of the effect of residual deformation and stress is for the sake of simplification. However, taking into consideration the effect of residual deformation and stress is possible in a way similar to that of the strain hardening effect.

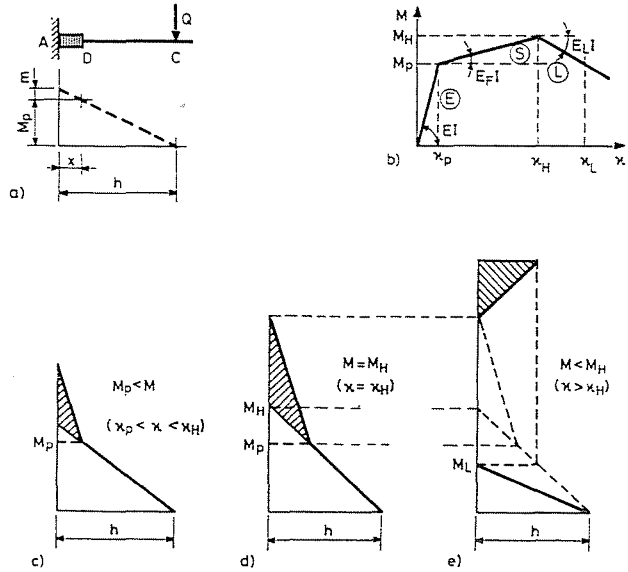

Fig. 23

The effect of plate buckling is investigated with the aid of the yield mechanism which is related to the load-displacement relationship. The fictive curvature pertaining to plate buckling can be determined in the form of

$$\varkappa_A = \frac{2\Theta_A}{x}$$

for cross section A,

where Θ_A is the rotation in cross section A determined with the aid of the yield mechanism,

x is the length of the zone (L).

The fictive curvature in cross section D is $\varkappa = 0$, and the curvature changes linearly (see Figure 23.e).

The relationship between the load on the rod end and the rotations is computed with the "moment-area" method.

For the elastic sections the reduced moment diagram is determined in the traditional way while for the inelastic sections in the following ways:

i) if $M_p < |M| < M_H$:

The moment exceeds the M_p value characteristic of the cross section, hence the hardening section develops. The moment diagram is modified by the rigidity characteristic ($E_S I$) of the hardening section S (see Figure 24.a, b).

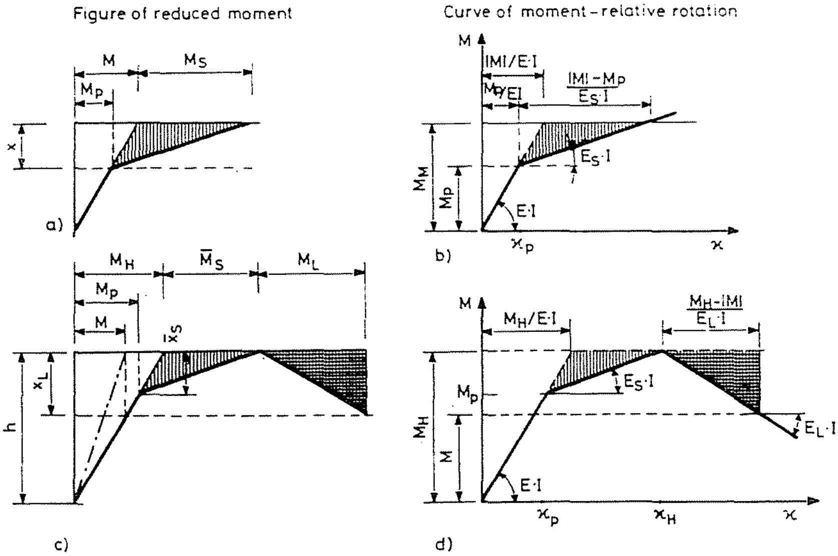

Fig. 24

From the similarity of perpendicularly shaded triangles:

$$\frac{M_S}{M} = \left[\frac{|M| - M_P}{E_S \cdot I} - \frac{|M| - M_P}{E \cdot I}\right] \frac{EI}{|M|}$$

$$M_S = M\left[1 - \frac{M_P}{|M|}\right]\left(\frac{E}{E_S} - 1\right)$$

ii) if $|M| < M_H$ ("descending part"):

The moment has reached the value M_H characteristic of the cross section, the plate buckling section develops. The moment diagram is modified by the rigidity characteristic ($E_L I$) of the plate buckling section L (see Fig. 24. d). From the similarity of perpendicularly shaded triangles:

$$|\overline{M}_S| = M_H\left[1 - \frac{M_P}{|M|}\right]\left(\frac{E}{E_S} - 1\right)$$

From the double shaded triangles:

$$\frac{X_L}{h} = \frac{M_H - |M|}{M_H} \qquad X_L = h\left[1 - \frac{|M|}{M_H}\right]$$

and

$$\frac{|M_L|}{M_H} = \frac{M_H - |M|}{E_L \cdot I} \cdot \frac{EI}{M_H}$$

$$|M_L| = M_H\left[1 - \frac{|M|}{M_H}\right]\frac{E}{E_L}$$

It should be noted that values $\overline{M}_S$, $\overline{x}_S$, h belong to the state $|M| = M_H$ and they are constant when computing the descending part.

With the aid of the model of the interactive hinge and zone the investigation of complex sections can also be undertaken.

7. Conclusions

The load-displacement relationship of I-section members built from plates has been investigated with plate buckling taken into account.

A yield mechanism formation has been determined to account for the effect of instability forms of the member, first of all that of plate buckling. The relationships pertaining to different yield mechanism formations have been determined for individual partial elements (flange plate, web plate) at different types of load (bending, compression). The compatibility of the yield mechanism formations developed for the individual partial elements has been fixed thus a description of the load-displacement relationship of the rod element became possible with the effect of plate buckling taken into account.

The effects of plate buckling and of member rotation have been experimentally verified in the "ascending" and "descending" range of the load-displacement curve. The formation of the buckling plate has been determined which proved the theoretical assumptions with the aid of measurement results.

The concept of the interactive hinge and zone have been introduced that take the changes developing in the member load-displacement relationship besides the effect of steel material hardening into account. These changes are brought about by plate buckling and member rotation. The interactive hinge constitutes the extension and generalization of the traditional plastic hinge while the interactive zone that of the plastic zone.

References

1. KAZINCZY, G.: Kísérletek befalazott tartókkal. (Experiments with clamped girders.) Betonszemle. Vol. II. (1914).
2. BEEDLE, L. S.: Ductility as a basis for steel design. "Engineering plasticity". Ed. Heyman, J., Leckie, F. A. Cambridge University Press, pp. 41—76. (1968).
3. HORNE, W. R.: Instability and the Plastic Theory of Structures. Transactions of the EIC. *4*, 31 (1960).

4. HORNE, M. R.—MEDLAND, J. C.: Collapse Loads of Steel Frameworks Allowing for the Effect of Strain-Hardening. Proc. of the Institution of Civil Engineers, Vol. 3. November. 1966.
5. MEYER, J. D.—GERSTLE, K. H.: Shakedown of Strain-Hardening Structures. Jrnl. of the Structural Division ST 1. 95 (1972).
6. RODERICK, J. W.: The load-deflection relationship for a partially plastic rolled steel joint. British Welding Journal, *1*, 78 (1954).
7. LAY, M. G.: A New Approach to Inelastic Structural Design. Proc. Instn. Civ. Engrs., *34*, 1 (1966).
8. TRANBERG, W.—SWANNELL, P.—MECK, J. L.: Frame Collapse Using Tangent Stiffness. Jrnl. of the Structural Division. March 1976.
9. LAY, M. G.: Residual Stresses in Steel Sections. Steel Construction. Jrnl. of the Australian Inst. of Steel Const. *3*, 2 (1969).
10. MALLOCK, A.: Note on the instability of tubes subjected to end pressure and on the folds in a flexible material. Proc. Royal Soc. Ser. A., Vol. 31. (1908).
11. HAAIJER, G.: Plate Buckling in the Strain-Hardening Range. Jrnl. of the Eng. Mech. Div., Vol. 83. EM2. April. (1957).
12. BEN KATO: Buckling Strength of the Plates in the Plastic Range. Publications of IABSE, Vol. 25. (1965).
13. CLIMENHAGA, J. J.—JOHNSON, P.: Moment-rotation curves for locally buckling beams. Jrnl. of Struct. Div. ASCE. Vol. 98 ST6. (1972).
14. KOROL, R. M.—SHERBOURNE: Strength predictions of plates in uniaxial compression. Journal of the Structural Division, ASCE, ST. 9. Sept. pp. 1965—1986. (1972).
15. MURRAY, M. W.: The behaviour of thin stiffened steel plates. Publications, IABSE, *3*, 191 (1973).
16. WALKER, A. C.—MURRAY, N. W.: A plastic collapse mechanism for compressed plates. Publications, IABSE, *35*, 217 (1975).
17. DAVIES, P.—KEMP, K. O.—WALKER, A. C.: An analysis of the failure mechanism of an axially loaded simply supported steel plate. Proc. Instn. Civ. Engrs., Part 2. *59*, 645 (1975).
18. MOUTY, J.: Calcul des charges ultimes des assemblages soudés de profils creux carrés et rectangulaires. Construction Métallique, No. 2. pp. 37—58. (1976).
19. PACKER, J. A.: Strut local buckling in trusses of rectangular hollow sections. Reg. Colloq. on Stability of Steel Structures, Proceeding. 1977. Hungary.
20. IVÁNYI, M.: Yield mechanism curves for local buckling of axially compressed members. Periodica Polytechnica, Civil Eng. *23*, 203 (1979).
21. IVÁNYI, M.: Moment-rotation characteristics of locally buckling beams. Periodica Polytechnica, Civil. Eng. *23*, 217 (1979).
22. IVÁNYI, M.: Interaction of Stability and Strength Phenomena in the Load Carrying Capacity of Steel Structures. Role of Plate Buckling. (In Hungarian). Doctor Techn. Sci. Thesis, Hung. Ac. Sci., Budapest, 1983.

Prof. Dr. Miklós IVÁNYI H-1521 Budapest